Monte Carlo simulation method for the Enskog equation

José María Montanero and Andrés Santos
Departamento de Física, Universidad de Extremadura, E-06071 Badajoz, Spain
(Received 31 October 1995)

A Monte Carlo simulation method to numerically solve the Enskog equation for a hard-sphere fluid is proposed. The method is based on and extends Bird's direct simulation Monte Carlo method to solve the Boltzmann equation. The main modifications are (a) the two particles of a collision pair are taken from cells separated a distance equal to the diameter of the spheres; (b) the collision rate is enhanced by a factor that accounts for the spatial correlations. The method is applied to uniform shear flow and proved to be consistent with (i) the exact pressure tensor obtained from the Enskog equation at local equilibrium for large shear rates, (ii) the viscous heating equation, and (iii) the Navier-Stokes shear viscosity obtained from the Enskog equation. [S1063-651X(96)02007-7]

PACS number(s): 05.60.+w, 47.50.+d, 83.20.Jp, 02.70.Lq

I. INTRODUCTION

The Boltzmann equation [1,2] provides an adequate framework for the investigation of nonequilibrium properties of low-density gases. While continuum hydrodynamic equations are only useful in the regime of large systems and small gradients, i.e., $L \gg \ell_h \gg \lambda$ (where L is the size of the system, ℓ_h is a characteristic hydrodynamic length, and λ is the mean free path), the Boltzmann equation is meaningful even if L and/or ℓ_h are comparable to or smaller than λ. Exact solutions to the Boltzmann equation are rare [3], but a great deal of information can be obtained from simplified kinetic models [4] or from Monte Carlo simulation methods [5]. The latter have proved to be a flexible and efficient tool to study the properties of rarefied gases in a wide variety of physical situations [6].

The main limitation of the Boltzmann equation is its restriction to the regime $\ell_h, \lambda \gg \sigma$, where σ is the effective range of molecular interactions. In 1922, Enskog [1,2] modified the Boltzmann equation for hard spheres of diameter σ by introducing two crucial changes in the collision integral: (a) the difference in position between the centers of a colliding pair of molecules is taken into account; (b) the collision frequency is increased by a factor that accounts for the spatial correlations between the two colliding molecules. Although the Enskog theory ignores the possibility of correlations in the velocities before collision (*stosszahlansatz*), it leads to transport coefficients that are in good agreement with experimental and simulation values over a wide range of densities, including those for which $\lambda < \sigma$. In addition, the revised Enskog theory (RET) developed by van Beijeren and Ernst [7] supports both fluid and crystal equilibrium states [8]. Thus the RET has the potential of describing fluid, crystal, and metastable states near and far from equilibrium. However, the intricate mathematical structure of the Enskog equation has prevented its application to many interesting physical situations. As in the case of the Boltzmann equation, two strategies are in principle possible: kinetic models and simulation methods. Very recently, a simple kinetic model of the Enskog equation has been proposed [9] that retains its essential features. The objective of this paper is to present a Monte Carlo simulation method, based on Bird's method for the Boltzmann equation [5], but that is devised to solve the Enskog equation. Previous attempts by Alexander *et al.* [10] modified Bird's method so that the hard-sphere equation of state is obtained at all densities. However, the transport coefficients at high densities deviate significantly from those of the Enskog equation.

The organization of this paper is as follows. The Enskog theory is briefly introduced in Sec. II. The simulation method is described in Sec. III. As an illustration, the method is applied in Sec. IV to the time-dependent uniform shear flow at a high density. Finally, the results are discussed in Sec. V.

II. THE ENSKOG THEORY

Let $f(\mathbf{r},\mathbf{v},t)$ be the one-particle distribution function. From it one can obtain the number density n and the flow velocity $\mathbf{u}$ as

$$n(\mathbf{r},t) = \int d\mathbf{v}\, f(\mathbf{r},\mathbf{v},t), \tag{2.1}$$

$$n(\mathbf{r},t)\mathbf{u}(\mathbf{r},t) = \int d\mathbf{v}\,\mathbf{v} f(\mathbf{r},\mathbf{v},t). \tag{2.2}$$

A nonequilibrium temperature T can also be defined by

$$\tfrac{3}{2} n(\mathbf{r},t) k_B T(\mathbf{r},t) = \tfrac{1}{2} m \int d\mathbf{v}[\mathbf{v}-\mathbf{u}(\mathbf{r},t)]^2 f(\mathbf{r},\mathbf{v},t), \tag{2.3}$$

where k_B is the Boltzmann constant and m is the mass of a particle. The kinetic contributions to the pressure tensor P and the heat flux $\mathbf{q}$ are also velocity moments of f:

$$\mathsf{P}^k(\mathbf{r},t) = m \int d\mathbf{v}[\mathbf{v}-\mathbf{u}(\mathbf{r},t)][\mathbf{v}-\mathbf{u}(\mathbf{r},t)] f(\mathbf{r},\mathbf{v},t), \tag{2.4}$$

$$\mathbf{q}^k(\mathbf{r},t) = \tfrac{1}{2} m \int d\mathbf{v}[\mathbf{v}-\mathbf{u}(\mathbf{r},t)]^2 [\mathbf{v}-\mathbf{u}(\mathbf{r},t)] f(\mathbf{r},\mathbf{v},t). \tag{2.5}$$

Except in the low-density limit, the potential contributions to P and $\mathbf{q}$ are relevant. In general, they are expressed in terms of the two-particle distribution function.

Following arguments similar to those leading to the Boltzmann equation, Enskog introduced a kinetic equation for f in the case of a dense hard-sphere fluid [1,2,11]:

$$\left(\frac{\partial}{\partial t}+\mathbf{v}\cdot\frac{\partial}{\partial \mathbf{r}}\right)f(\mathbf{r},\mathbf{v},t)=\sigma^2\int d\mathbf{v}_1\int d\hat{\boldsymbol{\sigma}}\,\Theta(\hat{\boldsymbol{\sigma}}\cdot\mathbf{g})(\hat{\boldsymbol{\sigma}}\cdot\mathbf{g})[\chi(\mathbf{r},\mathbf{r}-\boldsymbol{\sigma})f(\mathbf{r},\mathbf{v}',t)f(\mathbf{r}-\boldsymbol{\sigma},\mathbf{v}_1',t)-\chi(\mathbf{r},\mathbf{r}+\boldsymbol{\sigma})f(\mathbf{r},\mathbf{v},t)f(\mathbf{r}+\boldsymbol{\sigma},\mathbf{v}_1,t)]. \tag{2.6}$$

Here $\Theta(x)$ is the Heaviside function, $\mathbf{g}\equiv\mathbf{v}-\mathbf{v}_1$, and the primes on the velocities denote postcollision values:

$$\mathbf{v}'=\mathbf{v}-(\hat{\boldsymbol{\sigma}}\cdot\mathbf{g})\hat{\boldsymbol{\sigma}},\mathbf{v}_1'=\mathbf{v}_1+(\hat{\boldsymbol{\sigma}}\cdot\mathbf{g})\hat{\boldsymbol{\sigma}}. \tag{2.7}$$

In the standard Enskog theory (SET) [1], $\chi(\mathbf{r},\mathbf{r}+\boldsymbol{\sigma})=\chi(n(\mathbf{r}+1/2\boldsymbol{\sigma}))$, where $\chi(n)$ is the equilibrium pair correlation function at contact corresponding to a *uniform* density n. In the revised Enskog theory [7], however, $\chi(\mathbf{r},\mathbf{r}+\boldsymbol{\sigma})$ is identified with the local equilibrium pair correlation function in a *nonuniform* state. In that case, χ is a functional of n that can be obtained via density functional theory [12]. The RET and the SET lead to different predictions in nonhomogeneous states. Therefore the difference between both theories is relevant in states far from equilibrium (namely, beyond the Navier-Stokes order in the case of single substances), as well as in equilibrium crystal and (metastable) glassy states.

A primary consequence of the Enskog theory is that it leads to a collisional transfer of momentum and energy that can be expressed in terms of f. The collisional contributions to the pressure tensor and the heat flux are, respectively [13],

$$\mathsf{P}^c(\mathbf{r},t)=\tfrac{1}{2}\sigma^3 m\int d\mathbf{v}\int d\mathbf{v}_1\int d\hat{\boldsymbol{\sigma}}\,\Theta(\hat{\boldsymbol{\sigma}}\cdot\mathbf{g})(\hat{\boldsymbol{\sigma}}\cdot\mathbf{g})^2\hat{\boldsymbol{\sigma}}\hat{\boldsymbol{\sigma}}\int_0^1 d\mu\,\chi(\mathbf{r}-(1-\mu)\boldsymbol{\sigma},\mathbf{r}+\mu\boldsymbol{\sigma})f(\mathbf{r}-(1-\mu)\boldsymbol{\sigma},\mathbf{v},t)f(\mathbf{r}+\mu\boldsymbol{\sigma},\mathbf{v}_1,t), \tag{2.8}$$

$$\mathbf{q}^c(\mathbf{r},t)=-\mathsf{P}^c(\mathbf{r},t)\cdot\mathbf{u}(\mathbf{r},t)+\tfrac{1}{2}\sigma^3 m\int d\mathbf{v}\int \mathbf{v}_1\int d\hat{\boldsymbol{\sigma}}\Theta(\hat{\boldsymbol{\sigma}}\cdot\mathbf{g})(\hat{\boldsymbol{\sigma}}\cdot\mathbf{g})^2(\hat{\boldsymbol{\sigma}}\cdot\mathbf{G})\hat{\boldsymbol{\sigma}}\int_0^1 d\mu\,\chi(\mathbf{r}-(1-\mu)\boldsymbol{\sigma},\mathbf{r}+\mu\boldsymbol{\sigma})$$
$$\times f(\mathbf{r}-(1-\mu)\boldsymbol{\sigma},\mathbf{v},t)f(\mathbf{r}+\mu\boldsymbol{\sigma},\mathbf{v}_1,t), \tag{2.9}$$

where in Eq. (2.9) $\mathbf{G}\equiv 1/2(\mathbf{v}+\mathbf{v}_1)$. Explicit expressions for the Navier-Stokes constitutive equations are obtained from the Chapman-Enskog method [1]:

$$\mathsf{P}^k=nk_BT\mathsf{I}-\eta_E^k(n,T)[\nabla\mathbf{u}+(\nabla\mathbf{u})^\dagger-\tfrac{2}{3}(\nabla\cdot\mathbf{u})\mathsf{I}], \tag{2.10}$$

$$\mathsf{P}=p(n,T)\mathsf{I}-\eta_E(n,T)[\nabla\mathbf{u}+(\nabla\mathbf{u})^\dagger-\tfrac{2}{3}(\nabla\cdot\mathbf{u})\mathsf{I}]$$
$$-\zeta_E(n,T)(\nabla\cdot\mathbf{u})\mathsf{I}, \tag{2.11}$$

$$\mathbf{q}^k=-\kappa_E^k(n,T)\nabla T, \tag{2.12}$$

$$\mathbf{q}=-\kappa_E(n,T)\nabla T, \tag{2.13}$$

where

$$p(n,T)=nk_BT[1+\tfrac{2}{3}\pi n\sigma^3\chi(n)], \tag{2.14}$$

$$\eta_E^k(n,T)=\frac{1}{\chi(n)}[1+\tfrac{4}{15}\pi n\sigma^3\chi(n)]\eta_B(T), \tag{2.15}$$

$$\zeta_E(n,T)=\tfrac{4}{9}n^2\sigma^4\chi(n)(\pi mk_BT)^{1/2}, \tag{2.16}$$

$$\eta_E(n,T)=\frac{1}{\chi(n)}[1+\tfrac{4}{15}\pi n\sigma^3\chi(n)]^2\eta_B(T)+\tfrac{3}{5}\zeta_E(n,T), \tag{2.17}$$

$$\kappa_E^k(n,T)=\frac{1}{\chi(n)}[1+\tfrac{2}{5}\pi n\sigma^3\chi(n)]\kappa_B(T), \tag{2.18}$$

$$\kappa_E(n,T)=\frac{1}{\chi(n)}[1+\tfrac{2}{5}\pi n\sigma^3\chi(n)]^2\kappa_B(T)+\tfrac{3}{2}\frac{k_B}{m}\zeta_E(n,T). \tag{2.19}$$

In these equations, η_B and κ_B are the shear viscosity and thermal conductivity, respectively, derived from the Boltzmann equation for hard spheres. Their values are [1]

$$\eta_B(T)=1.0160\times\tfrac{5}{16}\left(\frac{mk_BT}{\pi}\right)^{1/2}\sigma^{-2}, \tag{2.20}$$

$$\kappa_B(T)=1.0251\times\tfrac{15}{4}\frac{k_B}{m}\eta_B(T). \tag{2.21}$$

To Navier-Stokes order, there is no distinction between the SET and the RET, while to Burnett order they differ in two linear transport coefficients in the momentum flux [14].

It is convenient to define a mean free path λ for a hard-sphere fluid as χ^{-1} times its low-density value, i.e.,

$$\lambda(n)=\frac{\sigma}{\sqrt{2}\pi n\sigma^3\chi(n)}. \tag{2.22}$$

For a rarefied gas, $n\sigma^3\to 0$, $\chi(n)\to 1$, and $\sigma/\lambda\to 0$. In that limit, the Enskog equation (2.6) reduces to the Boltzmann equation for hard spheres. On the other hand, for a density as moderate as $n\sigma^3=0.2$, $\sigma\simeq 1.2\lambda$ and the nonlocal character of collisions plays an essential role.

III. ENSKOG SIMULATION MONTE CARLO (ESMC) METHOD

In the early 1960's, Bird [5] devised the so-called direct simulation Monte Carlo (DSMC) method to numerically solve the Boltzmann equation, having been applied since then to a wide range of phenomena in rarefied gases [6]. In addition to formal proofs [15–17], comparisons with known exact solutions of the Boltzmann equation [15,18,19] show the accuracy of the DSMC method.

In the DSMC method, a number of particles are placed in a volume split into cells of size ΔL sufficiently smaller than the mean free path λ and the hydrodynamic length ℓ_h (over which the hydrodynamic fields change appreciably). The positions and velocities of the particles are updated after a time step Δt sufficiently smaller than the mean free time $\tau=\lambda/\sqrt{2k_BT/m}$ and the hydrodynamic time $t_h=\ell_h/\sqrt{2k_BT/m}$. This is done in two stages. In the first stage (free-streaming), the particles move freely and those leaving the volume are reentered according to the chosen boundary conditions. In the second stage (collisions), particles within the *same* cell are randomly chosen as collision partners (according to the interaction law considered) and postcollision velocities are assigned. The DSMC method and the Boltzmann equation have the *apparent* inconsistency of yielding transport coefficients that depend on the features of the interaction [cf. Eqs. (2.20) and (2.21)], while the equation of state is that of an ideal gas ($p=nk_BT$). In order to remove this inconsistency in the special case of hard spheres, Alexander *et al.* [10] have recently modified the DSMC method in two aspects. First, the two particles of an accepted collision pair are displaced a certain vector distance $\pm\boldsymbol{\sigma}$ after the collision step. Second, the collision rate at a given cell (of density n) is enhanced by a factor $\chi(n)$. This modified method, the so-called consistent Boltzmann algorithm (CBA), leads to the correct equilibrium equation of state, Eq. (2.14), but yields transport coefficients that differ from those of the Enskog theory, except in the low-density limit. In fact, no claim is made in Ref. [10] of the CBA being a numerical solution of the Enskog equation.

Our objective is to extend the DSMC method to represent a numerical solution to the Enskog equation. Let V be the volume of the system, which is split into cells of typical size $\Delta L\ll\lambda,\ell_h$. Notice that at finite density ΔL could be comparable to or even smaller than σ, while in the low-density limit it is fully consistent to take $\Delta L\gg\sigma$. A number N of particles are introduced at $t=0$ with random positions and velocities sampled from the initial distribution function. In order to improve the statistics, N should be as large as possible, as happens with the DSMC method [5]. Thus N/V is not necessarily equal to the average density $\overline{n}$ of the physical system we want to simulate. In fact, the ratio $\gamma\equiv\overline{n}/(N/V)$ is a constant that has a technical character and can be chosen independently of the physical parameter $\overline{n}$. The coarse-grained local density of cell I is $n_I=(N_I/V_I)\gamma$, where N_I and V_I are the number of particles and volume of cell I, respectively. To update the positions and velocities a free-streaming stage and a collision stage are decoupled over a time step $\Delta t\ll\tau,t_h$, just as in the DSMC method and the CBA. The only difference lies in the treatment of the collision stage. For every particle $i=1,\ldots,N$ the following steps are taken.

(i) Choose at random with equiprobability a given direction $\hat{\boldsymbol{\sigma}}_i$.

(2) Choose at random with equiprobability a test particle j belonging to the cell J that contains the point $\mathbf{r}_i+\sigma\hat{\boldsymbol{\sigma}}_i$. In general, the cell J is different from the cell I containing the point $\mathbf{r}_i$.

(3) The probability of accepting the collision between particles i and j is equal to the collision rate times the time step:

$$\omega_{ij}=\sigma^2 4\pi\Theta(\hat{\boldsymbol{\sigma}}_i\cdot\mathbf{g}_{ij})(\hat{\boldsymbol{\sigma}}_i\cdot\mathbf{g}_{ij})\chi(\mathbf{r}_i,\mathbf{r}_i+\sigma\hat{\boldsymbol{\sigma}}_i)n_J\Delta t, \tag{3.1}$$

where $\mathbf{g}_{ij}\equiv\mathbf{v}_i-\mathbf{v}_j$. In the SET, $\chi(\mathbf{r}_i,\mathbf{r}_i+\sigma\hat{\boldsymbol{\sigma}}_i)=\chi(n_{I'})$, where the cell I' is the one containing the point $\mathbf{r}_i+\frac{1}{2}\sigma\hat{\boldsymbol{\sigma}}_i$. In the RET, $\chi(\mathbf{r}_i,\mathbf{r}_i+\sigma\hat{\boldsymbol{\sigma}}_i)$ must be computed from the knowledge of the density in all cells, $\{n_K\}$.

(4) If the collision is rejected, make $\mathbf{v}_i'=\mathbf{v}_i$ and go to step (III). Otherwise, assign to particle i the postcollision velocity $\mathbf{v}_i'=\mathbf{v}_i-(\hat{\boldsymbol{\sigma}}_i\cdot\mathbf{g}_{ij})\hat{\boldsymbol{\sigma}}_i$, once the collision stage has finished for all the particles. The role of particle j is to sample the velocity distribution in the cell J, so that its velocity remains unchanged.

(5) Take the next particle and repeat the process.

The physical quantities are evaluated at every cell by averaging over the particles inside that cell and also over an ensemble of $\mathcal{N}$ different realizations. In each realization, the local flow velocity, the local kinetic pressure tensor, and the local kinetic heat flux are, respectively,

$$\mathbf{u}_I=\frac{1}{N_I}\sum_{i\in I}\mathbf{v}_i, \tag{3.2}$$

$$\mathsf{P}_I^k=\frac{\gamma}{V_I}m\sum_{i\in I}(\mathbf{v}_i-\mathbf{u}_I)(\mathbf{v}_i-\mathbf{u}_I), \tag{3.3}$$

$$\mathbf{q}_I^k=\frac{\gamma}{V_I}\tfrac{1}{2}m\sum_{i\in I}(\mathbf{v}_i-\mathbf{u}_I)^2(\mathbf{v}_i-\mathbf{u}_I). \tag{3.4}$$

The local collisional pressure tensor and heat flux are [20]

$$\mathsf{P}_I^c=-\tfrac{1}{2}\frac{\gamma\sigma}{V_I\Delta t}m\sum_{i\in I}(\mathbf{v}_i'-\mathbf{v}_i)\hat{\boldsymbol{\sigma}}_i, \tag{3.5}$$

$$\mathbf{q}_I^c=-\mathsf{P}_I^c\cdot\mathbf{u}_I-\tfrac{1}{4}\frac{\gamma\sigma}{V_I\Delta t}m\sum_{i\in I}(v_i'^2-v_i^2)\hat{\boldsymbol{\sigma}}_i. \tag{3.6}$$

In the low-density limit ($\sigma/\lambda\to 0$), the size of the cells ΔL can be taken much larger than σ. Consequently, particle j in step III belongs to the same cell as particle i ($J=I$). In addition, $\chi\to 1$ and the probability ω_{ij} in Eq. (3.1) becomes

$$\omega_{ij}=4\pi\Theta(\hat{\boldsymbol{\sigma}}_i\cdot\mathbf{g}_{ij})(\hat{\boldsymbol{\sigma}}_i\cdot\mathbf{g}_{ij})\frac{N_I/V_I}{N/V}\frac{\Delta t}{\sqrt{2}\pi\lambda}, \tag{3.7}$$

where use has been made of Eq. (2.22). Thus in that limit our method is equivalent to Nanbu's scheme of the DSMC method [16].

IV. APPLICATION TO UNIFORM SHEAR FLOW

In order to assess the validity of the ESMC method described in the preceding section, we have applied it to the uniform shear flow (USF). This nonequilibrium state is characterized [21] by a constant density, a linear velocity profile $\mathbf{u}(\mathbf{r})=\mathsf{a}\cdot\mathbf{r}$, $a_{\alpha\beta}=a\,\delta_{x\alpha}\delta_{y\beta}$ (a being the constant shear rate), uniform temperature and pressure tensor, and zero kinetic heat flux. The appropriate boundary condition leading to this state is that of Lees and Edwards [22], which for one-particle distribution function reads [23]

$$\tilde{f}(\tilde{\mathbf{r}},\tilde{\mathbf{v}},t)|_{\tilde{y}=-L/2}=\tilde{f}(\tilde{\mathbf{r}},\tilde{\mathbf{v}},t)|_{\tilde{y}=+L/2}, \tag{4.1}$$

where $\tilde{\mathbf{r}}\equiv\mathbf{r}-\mathbf{a}\cdot\mathbf{r}t$, $\tilde{\mathbf{v}}\equiv\mathbf{v}-\mathbf{a}\cdot\mathbf{r}$, and $\tilde{f}(\tilde{\mathbf{r}},\tilde{\mathbf{v}},t)\equiv f(\mathbf{r},\mathbf{v},t)$. In Eq. (4.1), L is the size of the system along the y axis. Since there are no boundary layers in the USF, the value of L does not play any relevant role. Conservation of energy yields the heating equation

$$\frac{de}{dt}=-aP_{xy}, \tag{4.2}$$

where e is the internal energy density, which for hard spheres is $e=\frac{3}{2}nk_BT$. Equation (4.2) can be derived from the Liouville equation [21] and is therefore exact. It implies that the USF is a time-dependent state. In order to compensate for this viscous heating effect, a nonconservative drag force is usually introduced in molecular dynamics simulations [24]. Here, however, we prefer not to introduce such a thermostat since Eq. (4.2) provides us with an extra consistency test of our method. The USF (without thermostat) has been analyzed via molecular dynamics [25], the DSMC method [26], the Bhatnagar-Gross-Krook model kinetic equation [27], and the Boltzmann equation [28].

The identification of a hydrodynamic length and time is straightforward in the case of the USF:

$$\ell_h=\sqrt{2k_BT/m}\,a^{-1}, \tag{4.3}$$

$$t_h=a^{-1}. \tag{4.4}$$

Since the temperature increases in time, so does ℓ_h, while t_h remains constant. Alternatively, the hard-sphere mean free path λ is stationary but the mean free time τ decreases as time elapses. As a consequence, the uniformity parameter [2] $\lambda/\ell_h=\tau/t_h$ monotonically decreases and the system asymptotically tends towards that of (local) equilibrium.

We have solved the Enskog equation for the USF by applying the ESMC method. Since the density n is uniform (except for the fluctuations inherent to a Monte Carlo method), there is no difference between the SET and the RET, so that $\chi(\mathbf{r}_i,\mathbf{r}_i+\sigma\hat{\boldsymbol{\sigma}})n_J=\chi(n)n$ in step (3). We have chosen the rather large density $n\sigma^3=0.8$, which corresponds to $\sigma=14.3\lambda$ [29]; in that case $\eta_E^k/\eta_E\simeq 0.1$. The cells have been defined as layers of width ΔL orthogonal to the y axis. The numerical values of the technical parameters are $L=\sigma$, $N=10^5$, $\mathcal{N}=5$, $\Delta L=10^{-2}\sigma$, $\Delta t=1.17\times10^{-2}\tau$. Notice that the time step Δt is not a constant, but it decreases as the system evolves [26]. The initial distribution function has been that of local equilibrium,

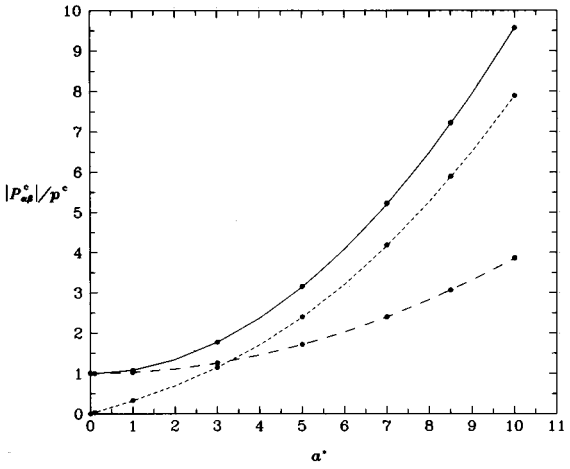

FIG. 1. Plot of $P^c_{xx}/p^c=P_{yy}/p^c$ (—), P^c_{zz}/p^c (– – –), and $-P^c_{xy}/p^c$ (- - -) as functions of a^* from Eq. (4.6). The circles represent the values obtained from the ESMC method (with $N=10^5$ particles and $\mathcal{N}=500$ realizations) using the distribution (4.5).

$$f(\mathbf{r},\mathbf{v},0)=n\left(\frac{m}{2\pi k_BT_0}\right)^{3/2}\exp[-m(\mathbf{v}-\mathbf{a}\cdot\mathbf{r})^2/2k_BT_0], \tag{4.5}$$

with two choices for the shear rate: $a=1.5\sqrt{2k_BT_0/m}/\sigma$ and $a=\sqrt{2k_BT_0/m}/\sigma$. In the particular case of Eq. (4.5), the Enskog expression for the collisional part of the pressure tensor, Eq. (2.8), becomes [13]

$$\begin{aligned}\mathsf{P}^c(t=0)=\tfrac{3}{4\pi}p^c(n)\int d\hat{\boldsymbol{\sigma}}\,\hat{\boldsymbol{\sigma}}\hat{\boldsymbol{\sigma}}\{&(1+a^{*2}\hat{\sigma}_x^2\hat{\sigma}_y^2)\\&\times[1-\mathrm{erf}(a^*\hat{\sigma}_x\hat{\sigma}_y/\sqrt{2})]\\&-\sqrt{\tfrac{2}{\pi}}a^*\hat{\sigma}_x\hat{\sigma}_y\mathrm{e}^{-a^{*2}\hat{\sigma}_x^2\hat{\sigma}_y^2/2}\},\end{aligned} \tag{4.6}$$

where $p^c(n)=\frac{2}{3}\pi n^2k_BT_0\sigma^3\chi(n)$ and $a^*\equiv a\sigma/\sqrt{2k_BT_0/m}$.

Three different tests have been applied to the simulation method: (i) consistency with Eq. (4.6), (ii) consistency with the exact equation (4.2), and (iii) consistency in the limit $\lambda/\ell_h\to 0$ with the Navier-Stokes pressure tensor obtained from the Enskog theory. In connection with the first test, we plot in Fig. 1 $|P^c_{\alpha\beta}|/p^c$ as a function of a^* from Eq. (4.6) and from the ESMC method (here with $\mathcal{N}=500$) using the distribution (4.5). The agreement is excellent. The simulation method correctly takes into account that, except for small values of a^*, the relative velocity of two colliding particles separated by a vector $\boldsymbol{\sigma}$ can be significantly different from zero. In the CBA, on the other hand, both particles of any colliding pair belong to the same cell, so that their velocities are sampled from the same distribution; consequently, $\mathsf{P}^c(t=0)=p^c(n)\mathsf{I}$.

Next, we compare in Fig. 2 the temperature $T(t)$ as obtained directly from the mean kinetic energy, Eq. (2.3), with that obtained from Eq. (4.2),

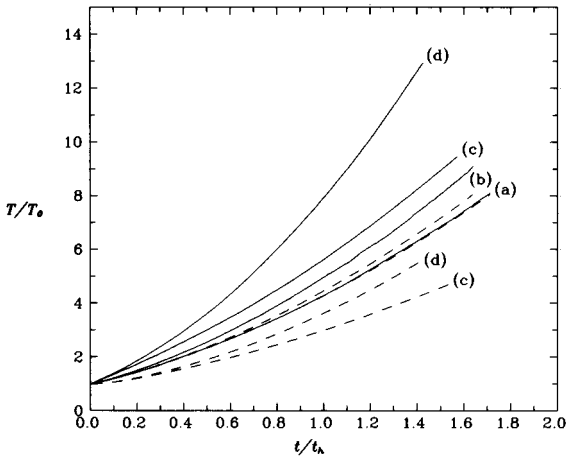

FIG. 2. Time dependence of the temperature as obtained directly from the mean kinetic energy (solid lines) and as obtained indirectly from Eq. (4.7) (dashed lines). They correspond to (a) the ESMC method with $\Delta L=10^{-2}\sigma$, (b) the ESMC method with $\Delta L=0.5\sigma$, (c) the CBA with $\Delta L=10^{-2}\sigma$, and (d) the CBA with $\Delta L=0.5\sigma$. The density is $n\sigma^3=0.8$ and the shear rate is $a^*=1$.

$$T(t)=T_0-\frac{2}{3}\frac{a}{nk_B}\int_0^t dt' P_{xy}(t'). \tag{4.7}$$

The results of Fig. 2 have been obtained from the CBA and the ESMC methods with $\Delta L/\sigma=10^{-2}$ and $\Delta L/\sigma=0.5$. While a strong inconsistency exists in the case of the CBA with both values of $\Delta L/\sigma$, in the ESMC method the two criteria to measure the temperature are practically indistinguishable if ΔL is sufficiently small ($\Delta L=10^{-2}\sigma=0.143\lambda$). For long times $P_{xy}\propto T^{1/2}$, so that $T^{1/2}$ becomes a linear function of time.

Finally, we perform the test (iii). The kinetic and collisional parts of the pressure tensor have been computed as a function of time. From the element $P_{xy}=P_{xy}^k+P_{xy}^c$, a time-dependent shear viscosity is defined as $\eta=-P_{xy}/a$; its kinetic part η^k is defined in a similar way. These shear viscosities, relative to their Navier-Stokes values given by the Enskog theory [Eqs. (2.15) and (2.17)], are plotted in Figs. 3 and 4. Rather than plotting them as functions of time, we have taken the (time-dependent) squared uniformity parameter $(\lambda/\ell_h)^2$ as the physically relevant variable; $(\lambda/\ell_h)^2$ is a decreasing function of t since ℓ_h increases (roughly linearly) with t. The abscissa is $(\lambda/\ell_h)^2$ instead of λ/ℓ_h because in the USF the first correction of the shear viscosity to its Navier-Stokes value is expected to be of second order in the uniformity parameter (super-Burnett order). After a transient regime of a few mean free times, the curves corresponding to the two different initial conditions practically coincide. This means that a hydrodynamic regime, independent of the initial preparation of the system, has been reached. In this hydrodynamic regime, the ratios η^k/η_E^k and η/η_E are, for a given density $n\sigma^3$, material functions of $(\lambda/\ell_h)^2$. Since in this section we are more interested in validating our simulation method than in analyzing rheological effects (for instance, shear thinning), the values of $(\lambda/\ell_h)^2$ considered in the simulations have been very small. From Figs. 3 and 4 it is evident that in the hydrodynamic regime η^k/η_E^k and η/η_E fluctuate around 1. The limit $\lambda/\ell_h\to 0$ is strictly unattainable in the USF because it requires an infinite amount of time. Also, the signal-to-noise ratio decreases in that limit so that the fluctuations increase.

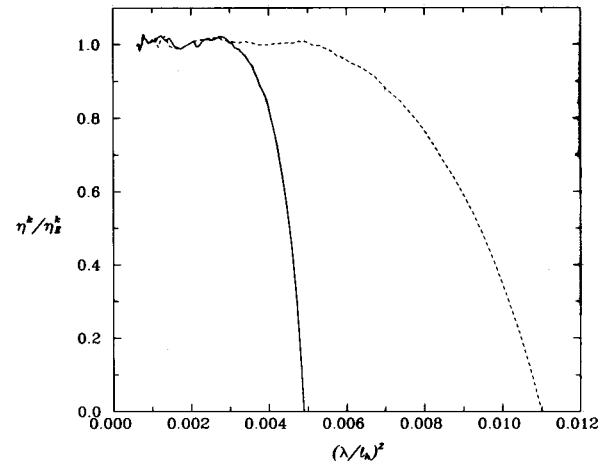

FIG. 3. Kinetic shear viscosity, relative to its Navier-Stokes value, as a function of the squared uniformity parameter $(\lambda/\ell_h)^2$. The density is $n\sigma^3=0.8$ and the shear rates are $a^*=1$ (solid line) and $a^*=1.5$ (dashed line).

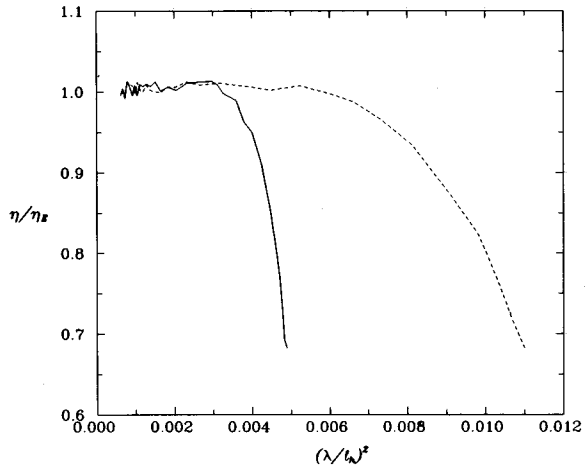

FIG. 4. The same as in Fig. 3, but for the total shear viscosity.

The diagonal elements of the pressure tensors, relative to their equilibrium values, are plotted in Figs. 5 and 6. Some of the comments about Figs. 3 and 4 also apply here. Extrapolation of the curves to $\lambda/\ell_h\to 0$ shows an excellent agreement with the predictions of the Enskog theory. Moreover, viscometric effects of Burnett order are clearly apparent. If we introduce the (dimensionless) viscometric functions $\Psi_1=(P_{yy}/p-P_{xx}/p)/(\lambda/\ell_h)^2$ and $\Psi_2=(P_{zz}/p-P_{yy}/p)/(\lambda/\ell_h)^2$, our simulation data yield $\Psi_1=-4.6$ and $\Psi_2=-22.8$ for $n\sigma^3=0.8$, while $\Psi_1=-2.569$ and $\Psi_2=0.218$ in the limit $n\sigma^3\to 0$ [1,26]. It is worthwhile to remark that Ψ_2 is small and positive at zero density, while it is large and negative at high density.

V. DISCUSSION

In this paper we have proposed a Monte Carlo simulation method that qualifies as a numerical solution of the Enskog equation. This Enskog simulation Monte Carlo method is

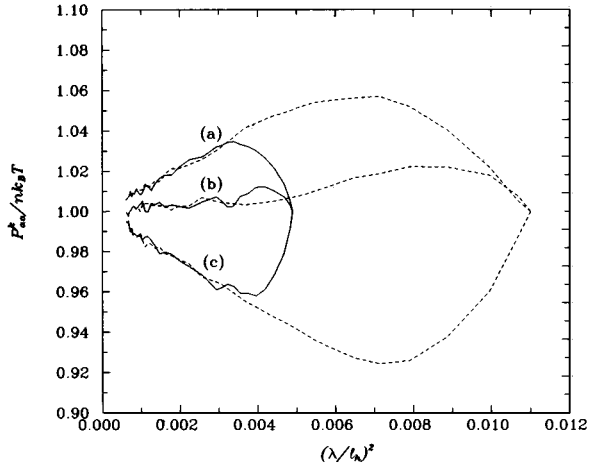

FIG. 5. Plot of (a) P^k_{xx}/nk_BT, (b) P^k_{yy}/nk_BT, and (c) P^k_{zz}/nk_BT as functions of the squared uniformity parameter $(\lambda/\ell_h)^2$. The density is $n\sigma^3=0.8$ and the shear rates are $a^*=1$ (solid line) and $a^*=1.5$ (dashed line).

based on and extends Bird's direct simulation Monte Carlo method to solve the Boltzmann equation. Since in the Boltzmann equation the collisions are local, the colliding partners in DSMC method are taken from the same cell. The Enskog equation, on the other hand, correctly takes into account that the centers of two colliding hard spheres are separated by a distance equal to the sphere diameter σ. Thus in the ESMC method each particle of a given colliding pair belongs, in general, to a different cell. In addition, the collision rate is enhanced by a factor χ that depends on the density field and the locations of both colliding particles. This factor can be implemented according to the standard Enskog theory or the revised Enskog theory. While the DSMC method is useful to study the regimes $\ell_h \sim \lambda$ and $\ell_h \ll \lambda$ (where λ is the mean free path and ℓ_h is the hydrodynamic length), but is restricted to $\sigma \ll \lambda, \ell_h$ (low-density limit), our method has access to the regimes $\sigma \sim \lambda$ and $\sigma \gg \lambda$ as well.

As an illustration, we have applied the ESMC method to the (unthermostatted) uniform shear flow. Since the ESMC method reduces, by construction, to the DSMC method in the low-density limit, we have carried out a stringent test by choosing a very high density ($n\sigma^3=0.8$), even though the Enskog theory is not expected to be adequate in that case. We have checked that the method (i) reproduces the exact pressure tensor obtained from the Enskog equation at local equilibrium for a wide range of shear rates, (ii) is consistent with the energy balance equation describing viscous heating, and (iii) yields the correct Enskog values for the elements of the pressure tensor in the Navier-Stokes limit. In the special case of the uniform shear flow, the factor χ is a constant, so that there is no distinction between the SET and the RET. Thus in this case the ESMC method is as computationally efficient as the DSMC method for comparable values of the ratio λ/ℓ_h. In fact, we have found [30] an excellent agreement between the simulation and the theoretical values of the shear viscosity over the whole range of densities. A similar agreement has been found in the cases of the thermal conductivity [31] and the self-diffusion coefficient [32] by using the homogeneous heat [33] and color [34] states, respectively.

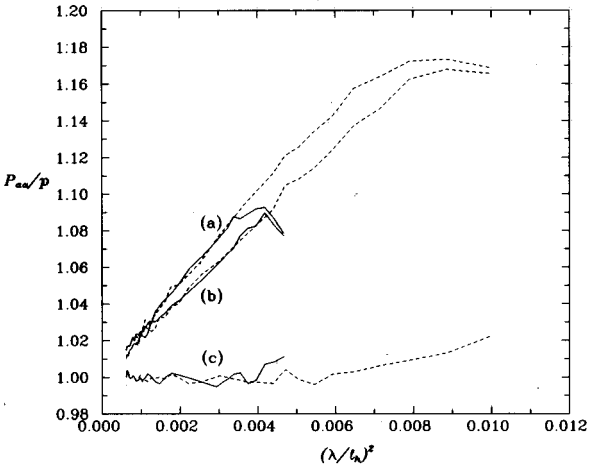

FIG. 6. The same as in Fig. 5, but for the diagonal elements of the total pressure tensor, relative to their equilibrium values.

It is known that the RET is asymptotically exact at short times, admits as stationary solutions the equilibrium distribution functions of both fluid and crystal, and predicts transport coefficients in excellent agreement with computer simulation values even for densities such that $\lambda < \sigma$. This means that the RET represents an adequate framework to investigate a wide variety of phenomena, including the kinetics of metastable states. From this point of view, it is obviously desirable to have an efficient, flexible, and accurate method to solve the Enskog equation. In our opinion, a good candidate for such a method is the one proposed in this paper.

Although our main motivation to develop the ESMC algorithm was to solve the Enskog equation rather than to be more efficient than molecular dynamics simulations, it is worthwhile to stress the computational advantage of the former in the regime of low and moderate densities. At low densities, hard-sphere molecular dynamics is inefficient because of the large number of possible collision partners within a neighborhood of a few mean free paths [10]. In fact, statistical inefficiency (defined as the long-sample limiting ratio of the observed variance to that expected for uncorrelated Gaussian statistics) is inversely proportional to density [35]. From the analysis of Ref. [10], we can estimate that, on a single processor computer, Monte Carlo algorithms (such as the DSMC, CBA, and ESMC) become more efficient than hard-sphere molecular dynamics at $n\sigma^3 \lesssim 0.3$. An extra advantage appears in states with a certain symmetry (e.g., spatial homogeneity, gradients along only one direction, etc.) that can be exploited to choose simple geometries for the cells in the Monte Carlo methods.

ACKNOWLEDGMENTS

The authors acknowledge the hospitality of the University of Florida for a visit in the summer of 1995 and are very grateful to Dr. J. W. Dufty for insightful discussions about the subject of this paper. Partial support from the DGICYT (Spain) through Grant No. PB94-1021 and PR95-153 and from the Junta de Extremadura–Fondo Social Europeo is acknowledged. The research of J.M.M. was supported by the Ministerio de Educación y Ciencia (Spain).

[1] S. Chapman and T. G. Cowling, *The Mathematical Theory of Non-Uniform Gases* (Cambridge University Press, Cambridge, England, 1970); J. H. Ferziger and H. G. Kaper, *Mathematical Theory of Transport Processes in Gases* (North-Holland, Amsterdam, 1972).
[2] J. R. Dorfman and H. van Beijeren, in *Statistical Mechanics. Part B: Time-Dependent Processes*, edited by B. J. Berne (Plenum Press, New York, 1977), pp. 65–179.
[3] A. Santos and V. Garzó, in *Rarefied Gas Dynamics 19*, edited by J. Harvey and G. Lord (Oxford University Press, Oxford, 1995), pp. 13–22.
[4] See, for instance, J. W. Dufty, in *Lectures on Thermodynamics and Statistical Mechanics*, edited by M. López de Haro and C. Varea (World Scientific, Singapore, 1990), pp. 166–181.
[5] G. A. Bird, *Molecular Gas Dynamics and the Direct Simulation of Gas Flows* (Clarendon Press, Oxford, 1994).
[6] *Rarefied Gas Dynamics 19*, edited by J. Harvey and G. Lord (Oxford University Press, Oxford, 1995), Chap. 7.
[7] H. van Beijeren and M. H. Ernst, Physica **68**, 437 (1973).
[8] T. R. Kirkpatrick, S. P. Das, M. H. Ernst, and J. Piasecki, J. Chem. Phys. **92**, 3768 (1990).
[9] J. W. Dufty, A. Santos, and J. J. Brey, Phys. Rev. Lett (to be published).
[10] F. J. Alexander, A. L Garcia, and B. J. Alder, Phys. Rev. Lett. **74**, 5212 (1995); in *25 Years of Non-Equilibrium Statistical Mechanics*, edited by J. J. Brey, J. Marro, J. M. Rubí , and M. San Miguel (Springer-Verlag, Berlin, 1995), pp. 82–90.
[11] P. Résibois and M. de Leener, *Classical Kinetic Theory of Fluids* (Wiley, New York, 1977), Chap. VI.
[12] M. Baus, J. Stat. Phys. **48**, 1129 (1987); J. Phys. Condens. Matter **2**, 2111 (1990); J. F. Lutsko and M. Baus, Phys. Rev. Lett. **64**, 761 (1990); Phys. Rev. A **41**, 6647 (1990).
[13] J. W. Dufty (unpublished).
[14] M. López de Haro and V. Garzó, Physica A **197**, 98 (1993).
[15] K. Nanbu, J. Phys. Soc. Jpn. **49**, 2042 (1980).
[16] K. Nanbu, in *Rarefied Gas Dynamics 15*, edited by V. Boffi and C. Cercignani (Teubner, Stuttgart, 1986), pp. 369–383.
[17] W. Wagner, J. Stat. Phys. **66**, 1011 (1992).
[18] C. Cercignani and S. Cortese, J. Stat. Phys. **75**, 817 (1994).
[19] J. M. Montanero and A. Santos, in *Rarefied Gas Dynamics 19*, edited by J. Harvey and G. Lord (Oxford University Press, Oxford, 1995), pp. 899–905.
[20] J. J. Erpenbeck and W. W. Wood, in *Statistical Mechanics. Part B: Time-Dependent Processes*, edited by B. J. Berne (Plenum Press, New York, 1977), pp. 1–40.
[21] J. W. Dufty, J. J. Brey, and A. Santos, in *Molecular-Dynamics Simulation of Statistical-Mechanical Systems*, edited by G. Ciccotti and W. G. Hoover (North-Holland, Amsterdam, 1986), pp. 294–303.
[22] A. W. Lees and S. F. Edwards, J. Phys. C **5**, 1921 (1972).
[23] J. W. Dufty, A. Santos, J. J. Brey, and R. F. Rodríguez, Phys. Rev. A **33**, 459 (1986).
[24] D. J. Evans and G. P. Morriss, *Statistical Mechanics of Nonequilibrium Liquids* (Academic Press, London, 1990).
[25] T. Naitoh and S. Ono, J. Chem. Phys. **70**, 4515 (1979).
[26] J. Gómez Ordóñez, J. J. Brey, and A. Santos, Phys. Rev. A **39**, 3038 (1989); **41**, 810 (1990).
[27] R. Zwanzig, J. Chem. Phys. **71**, 4416 (1979); A. Santos, J. J. Brey, and J. W. Dufty, Phys. Rev. Lett. **56**, 1571 (1986); A. Santos and J. J. Brey, Physica A **174**, 355 (1991).
[28] E. Ikenberry and C. Truesdell, J. Ration. Mech. Anal. **5**, 55 (1956); C. Truesdell and R. G. Muncaster, *Fundamentals of Maxwell's Kinetic Theory of a Simple Monatomic Gas* (Academic Press, New York, 1980); A. Santos and V. Garzó, Physica A **213**, 409 (1995); J. M. Montanero, A. Santos, and V. Garzó, Phys. Rev. E **53**, 1269 (1996).
[29] Here we have used the Carnahan-Starling equation of state [N. F. Carnahan and K. E. Starling, J. Chem. Phys. **51**, 635 (1969)], that yields $\chi(n)=(1-\pi/12n\sigma^3)/(1-\pi/6n\sigma^3)^3$.
[30] J. M. Montanero and A. Santos (unpublished).
[31] J. M. Montanero and A. Santos (unpublished).
[32] J. M. Montanero and A. Santos (unpublished).
[33] D. J. Evans, Phys. Lett. **91A**, 457 (1982); Phys. Rev. A **34**, 1149 (1986); M. J. Gillan and M. Dixon, J. Phys. C **16**, 869 (1983).
[34] D. J. Evans, W. G. Hoover, B. Failor, B. Moran, and A. J. C. Ladd, Phys. Rev. A **28**, 1016 (1983); D. J. Evans, R. M. Linden-Bell, and G. P. Morriss, Mol. Phys. **67**, 209 (1989).
[35] M. S. C. Reed and K. M. Flurchick, Comput. Phys. Commun. **81**, 56 (1994).